http://dx.doi.org/10.5012/bkcs.2014.35.11.3385

Selective Dephosphorylation by SCP1 and PP2A in Phosphorylated Residues of SMAD2

Jimoo Hong, Jinmo Sung, Dongsun Lee, Harikrishna Reddy R, and Young Jun Kim†,*

Department of Applied Biochemistry and †Nanotechnology Research Center, Konkuk University, Chung-ju 380-701, Korea
**E-mail: ykim@kku.ac.kr*
Received July 1, 2014, Accepted July 31, 2014

Key Words : Small CTD phosphatases, SCP1, SMAD2, Dephosphorylation, SMAD phosphatase

Protein phosphatase is important for cellular events, and a family of protein phosphatases, the so-called C-terminal domain (CTD) of RNA polymerase II (RNAPII) phosphatases, has recently attracted attention. The CTD is the largest subunit of RNAPII and consists of a tandem repeated heptapeptide ($Y_1S_2P_3T_4S_5P_6S_7$).[1] Seven active CTD phosphatases in the human genome are known and share the same catalytic domain architecture and DXDX(T/V) active site motif.[2] Small CTD phosphatase 1 (SCP1) dephosphorylates the fifth phosphorylated serine of $Y_1S_2P_3T_4S_5P_6S_7$ in the CTD[2] and has been renamed CTD small phosphatase 1 (CTDSP1). Small CTD phosphatase 2 (SCP2) and small CTD phosphatase 3 (SCP3) have a similar sequence, three-dimensional structure, and biochemical function to SCP1.[3] Small CTD phosphatases (SCPs, SCP1, SCP2, and SCP3) have been identified as a conserved regulators of neuronal stem cell development through silencing of neuronal genes *via* co-repression of the repressor element 1 (RE-1) silencing transcription factor/neuron-restrictive silencer factor (REST/NRSF).[4] In addition, several intracellular signaling pathways associated with SCPs have been reported in biological studies.[5] Some studies suggest that cell division cycle associated 3 (CdcA3)[6] and receptor-regulated SMADs (R-SMADs)[7] could be biological substrates of SCPs, and that SCPs are involved in signaling pathways of cell cycle regulation and cell differentiation.

Transformation growth factor β (TGF-β) and bone morphogenetic protein (BMP) signaling pathways are involved in cellular processes of differentiation, proliferation, motility, survival, and fate.[8,9] In these signaling pathways, SMADs are key components that control the transcription of TGF-β/BMP-targeted genes.[10] TGF-β and BMP cause the formation of a type1/type2 receptor complex through binding to their receptors and the subsequent phosphorylation of R-SMADs. The phosphorylation of R-SMADs triggers their translocation to the nucleus.[7] R-SMADs consist of five SMADs (SMADs 1, 2, 3, 5, and 8). SMADs 2 and 3 are activated by TGF-β, and SMADs 1, 5, and 8 are activated by BMP. R-SMADs have three structural features: Mad homology 1 (MH1) domain at the N-terminus, mad homology 2 (MH2) domain at the C-terminus, and a linker region.[10] The MH2 domain has a Ser-Ser-Xaa-Ser motif and these serine residues are phosphorylated. The phosphorylation of C-terminal Ser residues drives the activation of R-SMADs. The linker region contains several serine and threonine residues that are phosphorylated by several kinases.[7] Various phosphorylations of R-SMADs have been reported to affect their activity and cellular localization. The mechanisms of phosphorylation of R-SMADs are well known. The activation of R-SMADs has been also shown to be dependent on a proteasome pathway through interaction with selective WW-domain-containing E3 ubiquitin ligases.[10]

The reversible pathway of phosphorylation of R-SMADs is regulated by protein phosphatases. There are several protein phosphatases that could dephosphorylate phosphorylated residues within R-SMADs.[7] However, the mechanisms by which phosphatases regulate dephosphorylation are still unclear. Protein phosphatase Mg^{2+}/Mn^{2+}-dependent 1A (PPM1A; also known as PP2Cα) was first reported as a phosphatase of the SMAD2/3 tail SSXS motif. Overexpression of PPM1A resulted in decreased levels of tail-phosphorylated SMAD2/3.[11] PPM1A was also reported to act as a SMAD1 tail phosphatase.[12] Protein phosphatase 2A (PP2A) was reported to induce the dephosphorylation of SMAD3 tail serines under hypoxic conditions in the TGF-β pathway[13] and the dephosphorylation of both the C-terminus and the linker region of SMAD1 in the BMP pathway.[14] Myotubularin-related protein 4 (MTMR4) was also bound to SMAD2 and dephosphorylated SMAD2 tail serines.[15] Pyruvate dehydrogenase phosphatase (PDP), which is localized in mitochondria, was the first phosphatase to be reported as a SMAD1 tail phosphatase.[16] In addition, SCPs were proposed to be a SMAD1 tail phosphatase through depletion and overexpression studies.[17] SCP1 was also identified to regulate TGF-β and BMP signaling and improve the dephosphorylation of the linker region of SMAD1/2/3.[18] Recently, protein phosphatase Mg^{2+}/Mn^{2+}-dependent 1H (PPM1H; also known as NERRP-2C) was reported as a tail phosphatase of SMAD2.[19] These studies identifying phosphatases as R-SMAD tail phosphatases or R-SMAD linker phosphatases have generated controversy because of the inconsistency of cellular localization between the proposed phosphatases and phospho-SMAD in addition to irreproducible experimental results.[7]

More detailed studies of R-SMAD tail phosphatases and linker phosphatases are needed to establish a clear under-

standing of the regulation mechanism of R-SMADs in TGF-β and BMP signal transduction. Most previous studies concerning this issue were based on cell biological approaches; therefore, other evaluation methods should be used to determine which phosphatase is responsible for the dephosphorylation of the linker or tail region of R-SMADs. Among other methods, enzyme kinetics could provide important information because of its simplicity, although it has intrinsic limitations. We are thus able to acquire useful insight for the enzymatic and biochemical preference of SCPs and PP2A for a phosphorylated serine/threonine residue within the linker region or tail region of R-SMADs through enzyme kinetics.

In this study, we selected a sequence (supplementary Table 1) of 13 phosphopeptides originating from SMAD2 that were reported in HPRD and had the sequence synthesized by a commercial supplier. Among them, 3 phosphopeptides (S2, T8, and S110) were located in the MH1 domain and 5 phosphopeptides (S458, S460, S464, S465, and S467) were located in the MH2 domain of SMAD2. The other 5 phosphopeptides (T220, S240, S245, S250, and S260) are located in the linker region of SMAD2. We evaluated the specific activity of SCP1 and PP2A Cα with the 13 phosphopeptides of SMAD2 under reaction conditions originating from previous reports[2,20] to compare the relative activities. SCP1 had the highest specific activity against S250 and the second highest specific activity against S458 (Fig. 1(a)). The measured values were higher than the specific activity of SCP1 against CTD phosphopeptide (~20 μmol/min/mg) which was used in previous report[2] as a positive control. The specific activities against T8, S240, S245, and S467 are lower than 10 μmol/min/mg and the activities against S2, S110, T220, S260, S460, S464, and S465 are comparable to the specific activity against RRAT(p)VA peptide (~0 μmol/min/mg), included as a negative control. Interestingly, the specific activity against T8 and T220 was lower even though they have the PXS(p)P motif. PP2A had the highest specific activity against S460 and the second highest specific activity against S464 (Fig. 1(b)). PP2A showed no specific activity against the CTD phosphopeptide as a negative control. The activity against T220 was lower than 10 μmol/min/mg and the specific activities against the other phosphopeptides were almost zero. According to a previous study[20] for PP2A activity against the RRAT(p)VA peptide, PP2A Cα had a specific activity of 10.89 ± 2.44 μmol/min/mg, which was reconfirmed in this study when PP2A Cα was included as a positive control. Therefore, the specific activities of PP2A for S460 and S454 are comparable to that of the RRAT(p)VA peptide. These results indicate that SCP1 may be specific for the S250 dephosphorylation in the linker region of SMAD2 and for the S458 dephosphorylation in the tail region of SMAD2, but PP2A may be specific for the S460 dephosphorylation in the tail region of SMAD2 and for the S464 dephosphorylation in the SSXS motif of SMAD2.

To investigate which phosphorylated residue of SMAD2 is specific for SCP1, we determined the kinetic constants of SCP1 against 13 phosphopeptides of SMAD2. We initially

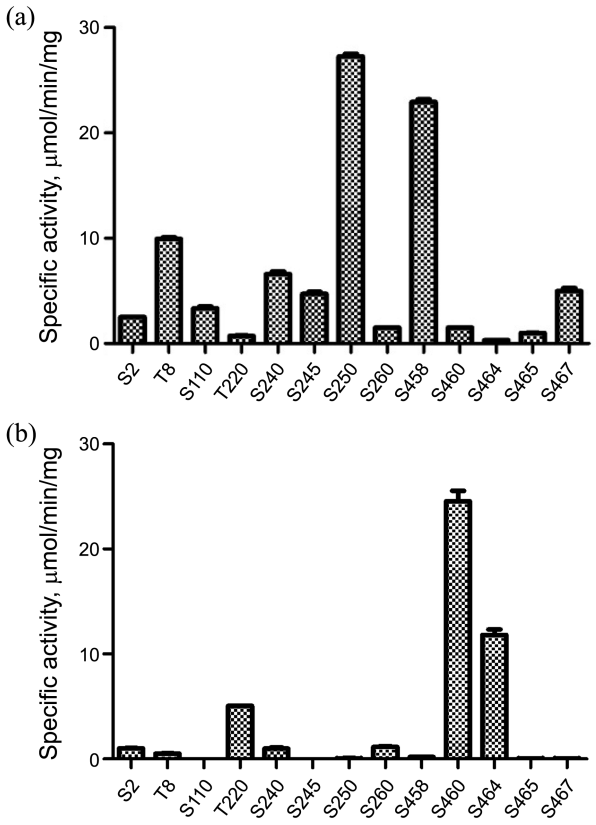

Figure 1. Selective dephosphorylation by SCP1 and PP2A Cα of phosphopeptides of SMAD2. (a) Specific activity of 35 ng SCP1 against 500 μM SMAD2 phosphopeptides incubated at 37 °C for 10 min. The data were the average of three independent measurements ± S.D. (b) Specific activity of 52.5 ng of PP2A Cα against 500 μM SMAD2 phosphopeptides incubated at 37 °C for 10 min. The data were the average of three independent measurements ± S.D.

used experimental conditions of pH 5.5, 37 °C, 5–100 ng of SCP1, and 10 min, which provided a steady state for SCP1. We observed the kinetic constant of SCP1 against the CTD phosphopeptide (14mer, YSPTSPSYSPTS(p)PS) for comparison. We measured the kinetic parameters of SCP1 with 13 phosphopeptides of SMAD2 and the data were fit to the Michaelis-Menten equation using PRISM software. The calculated kinetic constants of SCP1 are summarized in Table 1. The K_m value for T8, S245, S250, S458, and S467 was comparable to the K_m value of the CTD phosphopeptide (0.22 ± 0.075 mM). The k_{cat} values of S250 and S458 were similar to the value for CTD phosphopeptide (1.232 ± 0.189 s^{-1}). Although the k_{cat} value of S110 was quite high, we were not able to conclude that SCP1 has a high turnover rate for S110 because the standard deviation was too high. The measurements for S2, T220, S464, and S465 were out of the detection range because they did not provide the proper saturation curves for the Michaelis-Menten equation. To validate the efficiency of enzymatic catalysis for synthetic phosphopeptides of SMAD2, the specificity constants (k_{cat}/K_m, $s^{-1}mM^{-1}$) were calculated from the binding affinity (K_m) and turnover rate (k_{cat}). The k_{cat}/K_m value for the CTD phosphopeptide was 5.600 ± 1.587 $s^{-1}mM^{-1}$. The specificity

Table 1. Steady-State Kinetic Characterization of SCP1. The data represent the average value of three independent measurements ± S.D.[a] ND=Not detectable

Peptides	K_m (mM)	k_{cat} (s^{-1})	k_{cat}/K_m ($s^{-1}mM^{-1}$)
S2	ND[a]	ND	ND
T8	0.117 ± 0.024	0.048 ± 0.004	0.407 ± 0.165
S110	11.14 ± 9.76	3.090 ± 2.523	0.277 ± 0.258
T220	ND	ND	ND
S240	1.801 ± 1.741	0.832 ± 0.566	0.462 ± 0.325
S245	0.195 ± 0.058	0.182 ± 0.020	0.933 ± 0.343
S250	0.279 ± 0.037	1.447 ± 0.078	5.195 ± 2.116
S260	1.709 ± 0.225	0.250 ± 0.023	0.146 ± 0.102
S458	0.305 ± 0.050	1.185 ± 0.082	3.885 ± 1.640
S460	2.721 ± 0.689	0.356 ± 0.070	0.131 ± 0.102
S464	ND	ND	ND
S465	ND	ND	ND
S467	0.187 ± 0.054	0.285 ± 0.035	1.527 ± 0.648

Table 2. Steady-State Kinetic Characterization of PP2A Cα. The data represent the average value of three independent measurements ± S.D.[a] ND=Not detectable

Peptides	K_m (mM)	k_{cat} (s^{-1})	k_{cat}/K_m ($s^{-1}mM^{-1}$)
S2	3.403 ± 1.188	0.501 ± 0.140	0.147 ± 0.118
T8	ND[a]	ND	ND
S110	ND	ND	ND
T220	0.417 ± 0.054	0.604 ± 0.035	1.448 ± 0.648
S240	ND	ND	ND
S245	ND	ND	ND
S250	ND	ND	ND
S260	1.558 ± 0.390	0.314 ± 0.054	0.202 ± 0.138
S458	ND	ND	ND
S460	0.642 ± 0.238	2.777 ± 0.543	4.326 ± 2.282
S464	2.157 ± 0.549	4.179 ± 0.795	1.937 ± 1.448
S465	ND	ND	ND
S467	ND	ND	ND

constants of SCP1 for S250 (5.195 ± 2.116 $s^{-1}mM^{-1}$) and S458 (3.885 ± 1.640 $s^{-1}mM^{-1}$) are similar to the range of k_{cat}/K_m values for the CTD phosphopeptide. Thus, SCP1 is very specific for the dephosphorylation of S250 and S458. The specificity for S250 and S458 resulted from the relatively strong binding affinity (low K_m value) to SCP1 and higher turnover rate (k_{cat} value). The specificity constant for S467 (1.527 ± 0.648 $s^{-1}mM^{-1}$) was the third highest. Interestingly, T8 and T220 had very low specificity constants. This result was different from our speculation based on a crystallization study[2] of the complex of SCP1 and phosphopeptides of the CTD heptad repeat in RNAPII.

In contrast, we measured the kinetic constants of PP2A against 13 phosphopeptides of SMAD2 under the certain steady-state condition of pH 8.4, 37 °C, 5–60 ng of PP2A, and 10 min. The kinetic constants of PP2A are summarized in Table 2. PP2A had measurable K_m and k_{cat} values for S2, T220, S260, S460, and S464. However, the kinetic constants for T8, S110, S240, S245, S250, S465, and S467 could not be determined because they were out of the detection range. The specificity constants (k_{cat}/K_m, $s^{-1}mM^{-1}$) of PP2A for S460, S464, and T220 were 4.326 ± 2.282 $s^{-1}mM^{-1}$, 1.937 ± 1.448 $s^{-1}mM^{-1}$, and 1.448 ± 0.648 $s^{-1}mM^{-1}$, respectively. S2 and S260 showed very low specificity constants (0.147 ± 0.118 $s^{-1}mM^{-1}$ and 0.202 ± 0.648 $s^{-1}mM^{-1}$, respectively). Therefore, PP2A is relatively specific for the dephosphorylation of S460, S464, and T220. The specificity for S460 and T220 was derived from the relatively strong binding affinity (K_m value) to PP2A, whereas the specificity for S460 and S464 was derived from the relatively increased turnover rate (k_{cat} value). This result is quite similar to our findings for the relative specific activity of PP2A in Figure 1(b).

Although approaches using synthetic phosphopeptides are unable to show the 3-dimensional specificity of a phosphatase for a phosphorylated residue of a substrate, they are beneficial for providing essential information regarding enzymatic specificity. We selected enzyme kinetic characterization *in vitro* to evaluate the specificity of SCP1 and PP2A using synthetic phosphopeptides of SMAD2 because enzyme kinetics provides a basic and simple explanation for the preference of an enzyme for a substrate. Based on our kinetic characterization, we found that SCP1 is most specific for the dephosphorylation of S250 within linker region of SMAD2. We also found that PP2A is most specific for the dephosphorylation of S460 within the tail region of SMAD2. Thus, SCP1 and PP2A have selective specificity against phosphorylated sites of SMAD2. In conclusion, SCP1 and PP2A selectively dephosphorylate phosphorylated residues within the linker and tail region of SMAD2 and they dephosphorylate different residues within the tail or linker region of R-SMADs, respectively. Thus, SCP1 may be a linker phosphatase, but PP2A may be a tail phosphatase for R-SMADs.

Experimental Section

Materials. *para*-Nitrophenyl phosphate (pNPP), malachite green oxalate salt, ammonium molybdate tetrahydrate, and other general reagents were obtained from Sigma-Aldrich (St. Louis, USA). The protein phosphatase 2A C subunit (human recombinant; L309 deletion, PP2A Cα) was purchased from Cayman Chemical Co. (Ann Arbor, USA).

Preparation of Human Recombinant SCP1 and its Purification. The pET 21a(+)/N $SCP1^{76\text{-}261}$/His vector was introduced into the *E. coli* Rosetta 2 (DE3) strain. After an OD_{600} value of 0.6 was achieved, the *E. coli* culture was transferred to a pre-cooled incubator at 16 °C and the recombinant protein was induced with 0.4 mM isopropyl-β-D-thiogalactopyranoside (IPTG). The human recombinant SCP1 was expressed and purified by using a previously described protocol.[2]

Synthesis of Phosphopeptides. The phosphopeptides generated from SMAD2 based on the phosphorylation position reported in the Human Protein Reference Database

(HPRD) were synthesized by FMOC solid phase peptide synthesis using ASP48S and purified by reverse phase HPLC using a Vydac Everest C_{18} column (Peptron Inc., Daejeon, Korea). The sequences of the synthetic phosphopeptides are summarized in Supplementary Table 1.

Phosphatase Assays. SCP1-catalysed dephosphorylation of the phosphorylated substrate was performed as previously described[2] with minor modifications. Assays were conducted at 37 °C in a buffer consisting of 50 mM sodium acetate (pH 5.5), 20 mM $MgCl_2$, 5 μM-1mM phosphopeptides, and 5–100 ng of wild-type or mutant SCP1. PP2A Cα-catalyzed dephosphorylation of the phosphorylated substrate was performed as previously described.[20] Assays were conducted at 37 °C in a buffer consisting of 40 mM Tris-HCl (pH 8.4), 34 mM $MgCl_2$, 4 mM EDTA, 2 mM DTT, 0.05 mg/mL BSA, 5 μM-1 mM phosphopeptides, and 5–60 ng of PP2A Cα. Phosphate release was quantitated by using a malachite green-based colorimetric assay for inorganic phosphate by measuring the absorbance at 620 nm. The malachite green solution and inorganic phosphate standards were prepared as previously described.[21] To derive the K_M and k_{cat} values, the data were fit by nonlinear regression to the Michaelis-Menten equation using PRISM software.

Acknowledgments. This work was supported by Konkuk University.

Supporting Information. The sequence of synthesized phosphopeptides, abbreviations, and additional discussion are provided in the supplementary information.

References

1. Jasnovidova, O.; Stefl, R. *Wiley Interdisciplinary Reviews-Rna* **2013**, *4*, 1-16.
2. Zhang, Y.; Kim, Y.; Genoud, N.; Gao, J.; Kelly, J. W.; Pfaff, S. L.; Gill, G. N.; Dixon, J. E.; Noel, J. P. *Mol. Cell* **2006**, *24*, 759-770.
3. Yeo, M.; Lin, P. S. *Methods Mol. Biol.* **2007**, *365*, 335-346.
4. Yeo, M.; Lee, S. K.; Lee, B.; Ruiz, E. C.; Pfaff, S. L.; Gill, G. N. *Science* **2005**, *307*, 596-600.
5. R, H. R.; Kim, H.; Noh, K.; Kim, Y. J. *BMB Rep.* **2014**, *47*, 192-196.
6. Kim, Y. J.; Bahk, Y. Y. *Biochem. Biophys. Res. Commun.* **2014**, *448*, 189-194.
7. Bruce, D. L.; Sapkota, G. P. *FEBS Lett.* **2012**, *586*, 1897-1905.
8. Abdelmagid, S. M.; Belcher, J. Y.; Moussa, F. M.; Lababidi, S. L.; Sondag, G. R.; Novak, K. M.; Sanyurah, A. S.; Frara, N. A.; Razmpour, R.; Del Carpio-Cano, F. E.; Safadi, F. F. *Am. J. Pathol.* **2014**, *184*, 697-713.
9. Bae, J. S.; Gutierrez, S.; Narla, R.; Pratap, J.; Devados, R.; van Wijnen, A. J.; Stein, J. L.; Stein, G. S.; Lian, J. B.; Javed, A. *J. Cell Biochem.* **2007**, *100*, 434-449.
10. Massague, J.; Seoane, J.; Wotton, D. *Genes Dev.* **2005**, *19*, 2783-2810.
11. Lin, X.; Duan, X.; Liang, Y. Y.; Su, Y.; Wrighton, K. H.; Long, J.; Hu, M.; Davis, C. M.; Wang, J.; Brunicardi, F. C.; Shi, Y.; Chen, Y. G.; Meng, A.; Feng, X. H. *Cell* **2006**, *125*, 915-928.
12. Duan, X.; Liang, Y. Y.; Feng, X. H.; Lin, X. *J. Biol. Chem.* **2006**, *281*, 36526-36532.
13. Heikkinen, P. T.; Nummela, M.; Leivonen, S. K.; Westermarck, J.; Hill, C. S.; Kahari, V. M.; Jaakkola, P. M. *J. Biol. Chem.* **2010**, *285*, 3740-3749.
14. Bengtsson, L.; Schwappacher, R.; Roth, M.; Boergermann, J. H.; Hassel, S.; Knaus, P. *J. Cell Sci.* **2009**, *122*, 1248-1257.
15. Yu, J.; He, X.; Chen, Y. G.; Hao, Y.; Yang, S.; Wang, L.; Pan, L.; Tang, H. *J. Biol. Chem.* **2012**, *288*, 79-88.
16. Chen, H. B.; Shen, J.; Ip, Y. T.; Xu, L. *Genes Dev.* **2006**, *20*, 648-653.
17. Knockaert, M.; Sapkota, G.; Alarcon, C.; Massague, J.; Brivanlou, A. H. *Proc. Natl. Acad. Sci. USA* **2006**, *103*, 11940-11945.
18. Sapkota, G.; Knockaert, M.; Alarcon, C.; Montalvo, E.; Brivanlou, A. H.; Massague, J. *J. Biol. Chem.* **2006**, *281*, 40412-40419.
19. Shen, T.; Sun, C.; Zhang, Z.; Xu, N.; Duan, X.; Feng, X. H.; Lin, X. *Cell Res.* **2014**, *24*, 727-741.
20. Ikehara, T.; Shinjo, F.; Ikehara, S.; Imamura, S.; Yasumoto, T. *Protein Expr. Purif.* **2006**, *45*, 150-156.
21. Taylor, G. S.; Dixon, J. E. *Methods Mol. Biol.* **2004**, *284*, 217-227.